JOC Article
pubs.acs.org/joc

Isolation, Structure Elucidation, and Antitumor Activity of Spirohexenolides A and B

MinJin Kang, Brian D. Jones, Alexander L. Mandel, Justin C. Hammons, Antonio G. DiPasquale, Arnold L. Rheingold, James J. La Clair, and Michael D. Burkart*

Department of Chemistry and Biochemistry, University of California, San Diego, 9500 Gilman Drive, La Jolla, California 92093

mburkart@ucsd.edu

Received August 25, 2009

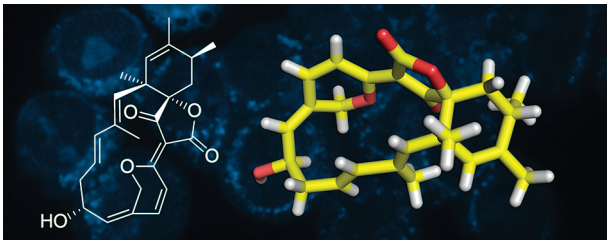

In this report, we describe the discovery of a pair of bioactive spirotetronates, spirohexenolides A (**1**) and B (**2**), that arose from the application of mutagenesis, clonal selection techniques, and media optimization to strains of *Streptomyces platensis*. The structures of spirohexenolides A (**1**) and B (**2**) were elucidated through X-ray crystallography and confirmed by 1D and 2D NMR studies. Under all examined culture conditions, spirohexenolide A (**1**) was the major metabolite with traces of spirohexenolide B (**2**) arising in cultures containing increased loads of adsorbent resins. Spirohexenolide A (**1**) inhibited tumor cell growth with GI_{50} values spanning from 0.1 to 17 μM across the NCI 60 cell line panel. An increased activity was observed in leukemia (GI_{50} value of 254 nM in RPMI-8226 cells), lung cancer (GI_{50} value of 191 nM in HOP-92 cells), and colon cancer (GI_{50} value of 565 nM in SW-620 cells) tumor cells. Metabolite **1** was fluorescent and could be examined on a confocal fluorescent microscope with conventional laser excitation and filter sets. Time lapse imaging studies indicated that spirohexenolide A (**1**) was readily taken up by tumor cells, appearing through the cell immediately after dosing and subcellularly localizing in the lysosomes. This activity, combined with a unique selectivity in NCI 60 cancer cell line screening, indicates that **1** warrants further chemotherapeutic evaluation.

Introduction

Since its classification in 1956,[1] *Streptomyces platensis* has demonstrated a remarkable ability to produce biologically active polyketides including the dorrigocins,[2] the migrastatins,[3] the pladienolides,[4] leustroducin B,[5] TPU-0037,[6] platensimide A,[7] and platensimycin.[8] Many of these compounds,[9] including synthetic analogues,[10] have demonstrated potent activity against tumor progression, and an analogue of

(1) Tresner, H. D.; Backus, E. J. *Appl. Microbiol.* **1956**, *4*, 243–250.
(2) (a) Hochlowski, J. E.; Whittern, D. N.; Hill, P.; McAlpine, J. B. *J. Antibiot.* **1994**, *47*, 870–874. (b) Karwowski, J. P.; Jackson, M.; Sunga, G.; Sheldon, P.; Poddig, J. B.; Kohl, W. L.; Kadam, S. *J. Antibiot.* **1994**, *47*, 862–869.
(3) (a) Woo, E. J.; Starks, C. M.; Carney, J. R.; Arslanian, R.; Cadapan, L.; Zavala, S.; Licari, P. *J. Antibiot.* **2002**, *55*, 141–146. (b) Ju, J. H.; Lim, S. K.; Jiang, H.; Shen, B. *J. Am. Chem. Soc.* **2005**, *127*, 1622–1623. (c) Gaul, C.; Njardarson, J. T.; Shan, D.; Dorn, D. C.; Wu, K. D.; Tong, W. P.; Huang, X. T.; Moore, M. A.; Danishefsky, S. J. *J. Am. Chem. Soc.* **2004**, *126*, 11326–11337.
(4) (a) Asai, N.; Kotake, Y.; Niijima, J.; Fukuda, Y.; Uehara, T.; Sakai, T. *J. Antibiot.* **2007**, *60*, 364–369. (b) Mandel, A. L.; Jones, B. D.; La Clair, J. J.; Burkart, M. D. *Bioorg. Med. Chem. Lett.* **2007**, *17*, 5159–5164. (c) Kanada, R. M.; Itoh, D.; Nagai, M.; Niijima, J.; Asai, N.; Mizui, Y.; Abe, S.; Kotake, Y. *Angew. Chem., Int. Ed.* **2007**, *46*, 4350–4355.
(5) Kohama, T.; Maeda, H.; Sakai, J. I.; Shiraishi, A.; Yamashita, K. *J. Antibiot.* **1996**, *49*, 91–94.
(6) Furumai, T.; Eto, K.; Sasaki, T.; Higuchi, H.; Onaka, H.; Saito, N.; Fujita, T.; Naoki, H.; Igarashi, Y. *J. Antibiot.* **2002**, *55*, 873–880.
(7) Herath, K. B.; Zhang, C.; Jayasuriya, H.; Ondeyka, J. G.; Zink, D. L.; Burgess, B.; Wang, J.; Singh, S. B. *Org. Lett.* **2008**, *10*, 1699–1702.
(8) Wang, J.; Soisson, S. M.; Young, K.; Shoop, W.; Kodali, S.; Galgoci, A.; Painter, R.; Parthasarathy, G.; Tang, Y. S.; Cummings, R.; Ha, S.; Dorso, K.; Motyl, M.; Hayasuriya, H.; Ondeyka, J.; Herath, K.; Zhang, C.; Hernandez, L.; Allocco, J.; Basilio, A.; Tormo, J. R.; Genilloud, O.; Vicente, F.; Pelaez, F.; Colwell, L.; Lee, S. H.; Michael, B.; Felcetto, T.; Gill, C.; Silver, L. L.; Hermes, J. D.; Bartizal, K.; Barrett, J.; Schmatz, D.; Becker, J. W.; Cully, D.; Singh, S. B. *Nature* **2006**, *441*, 358–361.

Published on Web 11/02/2009 DOI: 10.1021/jo901826d

pladienolide D, E7107, has recently entered clinical trials.[11] Given this track record, we were interested in evaluating associated strains of *S. platensis* for the production of yet undiscovered polyketides.

Recently, genome sequencing studies suggest that the bacterial secondary metabolomes are far more complicated than previously recognized by evaluation of their natural product content.[12] This, combined with further genetic screening programs, suggests that only a fraction of the potential natural products produced in bacteria have been identified.[13] The cause for this lack in production is complex. First, media and environmental stimuli can contribute to bacterial secondary metabolism either up- or down-regulating the production of specific metabolites based on external cues or morphological reponses.[14] Second, evolutionary pressures are often key in regulating a microbe′s ability to access secondary metabolism.[15] Mutagenesis offers a strong potential to circumvent the lack in production,[16] as mutant strains can be directed, through associated screening efforts, to enhance production. In this study, we demonstrate how applications of such strain improvement techniques can be used to access the production of new metabolites.

Results

Our studies began by evaluating a panel of *S. platensis* strains from available culture collections. An antibiotic assay using the inhibition of *Bacillus subtilis* growth was eventually chosen (comparable methods have been used in the discovery of spirotetronate natural products[17]). Due to the presence of only traces of compound **1** from the parent strain (often less than 1 mg/L), we applied both UV irradiation and NTG (*N*-methyl-*N*′-nitrosoguanidine) chemical mutagenesis for strain improvement. From UV irradiation analysis, we identified three mutant strains, MJ1A (1A, Figure 1a), MJ2B (2B, Figure 1a), and MJ6 (6, Figure 1a), that displayed an increased zone of inhibition over their parent *S. platensis* strain MJ (wt, Figure 1a). Subsequent efforts led to the production of two stable morphologies of MJ1A noted as strains MJ1A1 and MJ1A2.[18] 16S rRNA gene sequence data indicated that MJ1A strain showed high sequence identity to *S. platensis* NBRC12901 (99%),[19a] *S. hygroscopicus* subsp. *glebosus* LMG 19950 (99%),[19b] *S. libani* subsp. *rufus* NBRC 15424 (99%),[19c] and *S. caniferus* NBRC 15389 (99%).[19d]

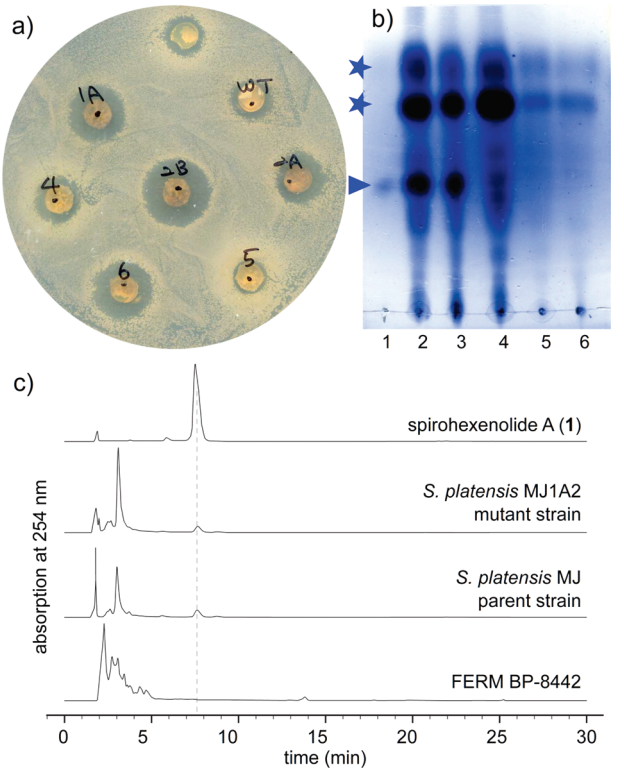

FIGURE 1. Production of metabolite **1** from *Streptomyces platensis* strains MJ1A1 and MJ1A2. (a) Ultraviolet light mutagenesis provided mutants with an increased ability to inhibit the growth of *Bacllius subtilis* 6633. An enhanced zone of growth inhibition was observed from mutant strains MJ1A, MJ2B, and MJ6 as compared to their parent strain (wt). (b) TLC analysis of extracts from *S. platensis* strains cultures. A direct comparison of crude extracts from these cultures indicates that metabolite **1** (lane 1) was enhanced in *S. platensis* strain MJ1A1 (lane 2) and strain MJ1A2 (lane 3), as compared to their parental strain (lane 4) or two morphologically different colonies of *S. platensis* FERM BP-8442 (lanes 5 and 6). An arrow denotes the position of metabolite **1** and stars denote the position of lipids and acylglycerides. The TLC observations were confirmed by preparative isolation, which after multiple repeats failed to return traces of **1** from cultures of the strains in lanes 5 and 6. (c) HPLC traces collected with UV detection at 254 nm confirmed the presence of **1** in both parent *S. platensis* MJ and mutant *S. platensis* MJ1A2 strains while not in *S. platensis* FERM BP-8442. The MIC of pure **1** against *Bacillus subtilis* was determined to be 12.25 μM (see the Experimental Section), therein supporting the viability of the screening procedure.

(9) Ju, J. H.; Rajski, S. R.; Lim, S. K.; Seo, J. W.; Peters, N. R.; Hoffmann, F. M.; Shen, B. *Bioorg. Med. Chem. Lett.* **2008**, *18*, 5951–5954.
(10) Metaferia, B. B.; Chen, L.; Baker, H. L.; Huang, X. Y.; Bewley, C. A. *J. Am. Chem. Soc.* **2007**, *129*, 2434–2435.
(11) Kotake, Y.; Sagane, K.; Owa, T.; Mimori-Kiyosue, Y.; Shimizu, H.; Uesugi, M.; Ishihama, Y.; Iwata, M.; Mizui, Y. *Nat. Chem. Biol.* **2007**, *3*, 570–575.
(12) (a) Li, M. H.; Ung, P. M.; Zajkowski, J.; Garneau-Tsodikova, S.; Sherman, D. H. *BMC Bioinf.* **2009**, *10*, 185. (b) Gulder, T. A.; Moore, B. S. *Curr. Opin. Microbiol.* **2009**, *12*, 252–260. (c) Jones, A. C.; Gu, L.; Sorrels, C. M.; Sherman, D. H.; Gerwick, W. H. *Curr. Opin. Chem. Biol.* **2009**, *13*, 216–223. (d) Udwary, D. W.; Zeigler, L.; Asolkar, R. N.; Singan, V.; Lapidus, A.; Fenical, W.; Jensen, P. R.; Moore, B. S. *Proc. Natl. Acad. Sci. U.S.A.* **2007**, *104*, 10376–10381.
(13) (a) Gust, B. *Methods Enzymol.* **2009**, *458*, 159–180. (b) Wilkinson, B.; Micklefield, J. *Nat. Chem. Biol.* **2007**, *3*, 379–386. (c) Baltz, R. H. *Antonie Van Leeuwenhoek*. **2001**, *79*, 251–259.
(14) van Wezel, G. P.; Krabben, P.; Traag, B. A.; Keijser, B. J.; Kerste, R.; Vijgenboom, E.; Heijnen, J. J.; Kraal, B. *Appl. Environ. Microbiol.* **2006**, *72*, 5283–5288.
(15) (a) te Poele, E. M.; Bolhuis, H.; Dijkhuizen, L. *Antonie Van Leeuwenhoek* **2008**, *94*, 127–143. (b) Demain, A. L. *Int Microbiol.* **1998**, *1*, 259–264. (c) Hopwood, D. A. *Philos. Trans. R. Soc. London, Ser. B* **1989**, *324*, 549–562.
(16) (a) Wang, L. Y.; Yun, B. S.; George, N. P.; Wendt-Pienkowski, E.; Galm, U.; Oh, T. J.; Coughlin, J. M.; Zhang, G.; Tao, M.; Shen, B. *J. Nat. Prod.* **2007**, *70*, 402–406. (b) Malina, H.; Tempete, C.; Robert-Gero, M. *J. Antibiot.* **1985**, *38*, 1204–1210. (c) Lee, S. D.; Park, S. W.; Oh, K. K.; Hong, S. I.; Kim, S. W. *Lett. Appl. Microbiol.* **2002**, *34*, 370–375. (d) Lyutskanova, D. G.; Stoilova-Disheva, M. A.; Peltekova, V. T. *Appl. Biochem. Microbiol.* **2005**, *41*, 165–168. (e) Kieser, T.; Bibb, M. J.; Buttner, M. J.; Chater, K. F.; Hopwood, D. A. *Practical Streptomyces Genetics*; The John Innes Foundation: Norwich, England, 2000. (f) Lalm, R.; Khanna, R.; Kaur, H.; Khanna, M.; Dhingra, N.; Lal, S.; Gartemann, K. H.; Eichenlaub, R.; Ghosh, P. K. *Crit. Rev Microbiol.* **1996**, *22*, 201–255. (g) Hopwood, D. A.; Chater, K. F. *Philos. Trans. R. Soc. London, Ser. B* **1980**, *290*, 313–328.
(17) (a) Schindler, P. W.; Zahner, H. *Eur. J. Biochem.* **1973**, *39*, 591–600. (b) Gary, N. D.; Bard, R. C. *J. Bacteriol.* **1952**, *64*, 501–512. (c) Sundaram, T. K.; Cazzulo, J. J.; Kornberg, H. L. *Biochim. Biophys. Acta* **1969**, *192*, 355–357.
(18) Pang, X. H.; Aigle, B.; Girardet, J. M.; Mangenot, S.; Pernodet, J. L.; Decaris, B.; Leblond, P. *Antimicrob. Agents Chemother.* **2004**, *48*, 575–588.

^{1}H NMR-guided fractionation was applied to extracts from cultures of the *S. platensis* MJ1A1 and *S. platensis* MJ1A2. Metabolite **1**, with a unique signature of olefinic protons in the NMR spectrum, was identified in the ethyl acetate (EtOAc) extract from both cultures. TLC analysis indicated that metabolite **1** (lane 1, Figure 1b) was more abundant in extracts from strains MJ1A1 (lane 2, Figure 1b) and MJ1A2 (lane 3, Figure 1b) than their parent strain *S. platensis* MJ (lane 4, Figure 1b). Control experimentation indicated that **1** also did not appear in related strains such as FERM BP-8442 (lanes 5 and 6, Figure 1b), indicating that the production of **1** was restricted to strains MJ1A1 and MJ1A2. Similarly, HPLC analyses using UV detection at 254 nm confirmed the presence of **1** in both parent (*S. platensis* strain MJ) and mutant strains but not in other strains of *S. platensis* (Figure 1c). While **1** was observed in parent (traces) and mutant extracts, TLC evidence (Figure 1b) indicates that the mutants offered a significant increase in production of **1** relative to their lipid content (lipids could not be detected under our HPLC methods).

After identification by ^{1}H NMR and MS analyses, small yellow needles of compound **1** were obtained by perfusion of a chloroform solution of **1** with benzene. Yellow plates were more effectively obtained by recrystallization from ethanol, mp 280−285 °C dec. Samples of these crystals were then evaluated by X-ray crystallography. The structure of **1** was refined to a final R1 of 4.6%. With use of anomalous copper dispersion effects,[20] absolute stereochemical information was obtained as depicted in Figure 2.

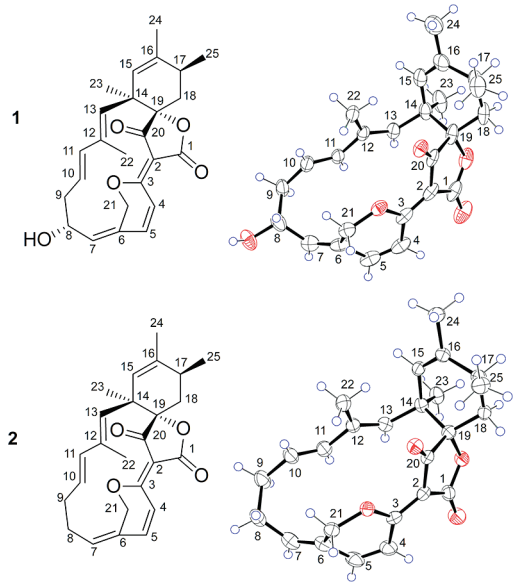

FIGURE 2. Structures of spirohexenolides A (**1**) and B (**2**), and corresponding ORTEP drawings of their X-ray crystal structures with ellipsoids drawn at the 50% probability level. The drawings represent absolute configuration as the Flack *x* parameter was 0.0(3).[20b]

Spectroscopic methods confirmed the crystal structure as follows. A molecular formula for **1** of $C_{25}H_{28}O_5$ was determined from high-resolution EI-MS analysis (*m*/*z* 408.1947, M^+, Δ 3.7 ppm). Strong absorption bands at 1754 and 1702 cm^{-1} in the FT-IR spectrum confirmed the presence of both ester and ketone groups, respectively.

An NMR data set including ^{1}H, ^{13}C, gCOSY, TOCSY, NOESY, ROESY, HMQC, HSQC, DEPT, and HMBC spectra was collected for spirohexenolide A (**1**) in $CDCl_3$ (Table 1). Twenty-five resonances were observed in the ^{13}C spectrum as expected from the HRMS data. The DEPT spectrum indicated sixteen protonated carbons including four methyl carbons, an oxymethylene, two aliphatic methylene carbons, an aliphatic methine, an oxymethine, and seven olefin methine carbons. Three of the nine quaternary carbons were observed in the olefin region for a total of ten olefinic carbon resonances, indicating five double bonds.

Three of the six remaining quaternary carbons appeared in the carbonyl region of the spectrum, one of which was the conjugated ketone at δ_C 196.0 and two of which appeared in the ester/lactone region at δ_C 169.3 and δ_C 165.7; this was supported by the carbonyl peaks in the FT-IR spectrum. The fourth was thought to be a quaternary center due to its upfield shift at δ_C 44.3. The two quaternary carbons at δ_C 100.8 and δ_C 89.2 remained ambiguous.

Analysis of the ^{1}H and gCOSY spectra of **1** (Figure 3a) revealed four spin systems. The first system began with the two downfield olefin methine protons H-4 (δ_H 7.44, d, 10.0 Hz) and H-5 (δ_H 7.02, d, 10.0 Hz). H-5 showed allylic coupling to oxymethylene proton H-21a (δ_H 4.73, d, 12.5 Hz), implicating a four-carbon subunit for this spin system with a junction at quaternary olefinic C-6. The J = 10.0 Hz coupling constant between H-4 and H-5 was consistent with a cis-olefin.

The second spin system comprised a linear subunit including olefinic methine H-7 (δ_H 5.72, d, 8.4 Hz), oxymethine H-8 (δ_H 4.60, m), aliphatic methylene pair H_2-9 ($\delta_{H\text{-}9a}$ 2.60, m, $\delta_{H\text{-}9b}$ 2.17, dt, 12.3, 10.6 Hz), olefinic methine H-10 (δ_H 5.55, ddd, 5.4, 10.6, 15.5 Hz), and olefinic methine H-11 (δ_H 5.69, d, 15.5 Hz). The J = 15.5 Hz coupling constant between H-10 and H-11 established the *E* configuration for the $\Delta^{10,11}$ olefin. The third spin system was an isolated two-resonance spin system including olefinic methine H-13 (δ_H 5.07, s) and vinyl methyl H_3-22 (δ_H 1.76, s), presumably connected via quaternary olefinic C-12.

The fourth spin system was a branched subunit beginning with olefinic methine H-15 (δ_H 5.29, s), which displayed allylic coupling to vinyl methyl H_3-24 (δ_H 1.76, s) and to aliphatic methine H-17 (δ_H 2.39, m). H-17 also coupled to methyl H_3-25 (δ_H 1.34, d, 7.2 Hz) and methylene pair H_2-18 ($\delta_{H\text{-}18a}$ 2.35, m, $\delta_{H\text{-}18b}$ 1.71, d, 13.6 Hz). The C-23 methyl group was not in any of the spin systems, indicating that it was attached to a quaternary center.

Figure 3a depicts several of the key HMBC correlations that validated the structure. The HMBC data confirmed the assignments of the C-3 and C-6 ^{13}C signals at δ_C 165.7 and δ_C 126.7, respectively, based on the correlations from H-4, H-5, and H-21a, all in the first spin system. Tethering of the first and second spin systems hinged on the HMBC correlation from H-5 and H-21b to olefinic methine C-7, suggesting quaternary C-6 as the junction. This C-3 to C-11 segment could be extended to include the CH-13/CH_3-22 system based on reciprocal HMBC correlations between olefinic H-11 and H-13 and their respective carbons. Quaternary olefinic C-12 (δ_C 136.2) was assigned

(19) (a) Shirling, E. B.; Gottlieb, D. *Int. J. Syst. Bacteriol.* **1968**, *18*, 279–392. (b) Kumar, Y.; Goodfellw, M. *Int. J. Syst. Evol. Microbiol.* **2008**, *58*, 1369–1378. (c) Skerman, V. B. D.; Mcgowan, V.; Sneath, P. H. A. *Int. J. Syst. Bacteriol.* **1980**, *30*, 225–420. (d) Preobrazhenskaya, T. P. *Int. J. Syst. Bacteriol.* **1986**, *36*, 573–576.

(20) (a) For an example, see: Niu, X. M.; Li, S. H.; Görls, H.; Schollmeyer, D.; Hilliger, M.; Grabley, S.; Sattler, I. *Org. Lett.* **2007**, *9*, 2437–2440. (b) For a definition, see: Flack, H. D. *Acta Crystallogr., Sect. A* **1983**, *39*, 876–881.

TABLE 1. ^{1}H, ^{13}C, gCOSY, NOESY, and HMBC NMR Data[g] for Spirohexenolide A (**1**) in $CDCl_3$

C/H no.	δ_H mult (*J* Hz)[a]	δ_C (mult)[b]	COSY[c]	NOESY[c]	HMBC[c,f]
1		169.3 (C)			
2		100.8 (C)			
3		165.7 (C)			
4	7.44 d (10.0)	120.3 (CH)	5	5	3,6
5	7.02 d (10.0, < 1)	142.1 (CH)	4,21a	4,7	3,6,7,21
6		126.7 (C)			
7	5.72 d (8.4)	139.3 (CH)	8	5,21b	5,21
8	4.60 m	69.3 (CH)	7,9a,9b	9a,9b,10	9
9a	2.60 m		8,9b,10	8,9b,10,11[e]	8,10,11
9b	2.17 dt (10.6, 12.3)	42.6 (CH_2)	8,9a,10	8,9a,10,11	8,10,11
10	5.55 ddd (5.4, 10.6, 15.5)	120.8 (CH)	9a,9b,11	8[d],9a,9b,13[e],21a,21b[d],22[d]	9,11,12
11	5.69 d (15.5)	140.9 (CH)	9a,10	9b,13	9,10,13,22
12		136.2 (C)			
13	5.07 s	134.8 (CH)	22	10,11,15[e],23[e]	11,14,15,22,23
14		44.3 (C)			
15	5.29 s	128.0 (CH)	17,24	13,23,24	13,14,17,19,24
16		133.4 (C)			
17	2.39 m	33.5 (CH)	15,18a,18b,25	18a,25	15,16,18,19,25
18a	2.35 m	33.3 (CH_2)	17,18b	17,18b,23	14,17,19,20,25
18b	1.71 d (13.6)		17,18a	18a,25	14,16,17,19,20,25
19		89.2 (C)			
20		196.0 (C)			
21a	4.73 d (12.5)	64.8 (CH_2)	5,21b	10,21b[d]	3,5,6,7
21b	4.57 d (12.5)		21a	7,10,21a	5,6,7
22	1.76 s	14.1 (CH_3)	13	10	11,12
23	1.19 s	27.2 (CH_3)		13,15,18a	13,14,15,19
24	1.76 s	22.0 (CH_3)	15	15,25	15,16,17,18
25	1.34 d (7.2)	19.6 (CH_3)	17	17,18b,24[d]	16,17,18

[a] ^{1}H NMR data were collected at 500 MHz. [b] ^{13}C NMR data were collected at 100 MHz. ^{13}C NMR multiplicities were determined by the DEPT spectrum. [c] gCOSY, HMBC, and NOESY spectra were collected at 800 MHz. [d] Overlapping signals detected [e] A weak crosspeak was detected. [f] HMBC data were collected with an evolution delay optimized for $^{2,3}J_{CH}$ = 8 Hz. [g] Spectra were collected at 296 K in $CDCl_3$.

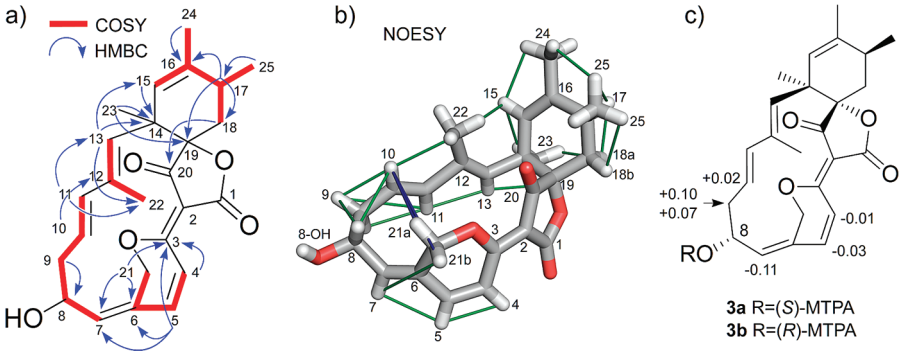

FIGURE 3. Select NMR data. (a) Key gCOSY and HMBC correlations for spirohexenolide A (**1**) and (b) Nuclear Overhauser effects identified through analysis of a NOESY spectrum as mapped on the X-ray crystal structure of **1**. Both proximal (green) and transannluar (blue) NOEs are shown. (c) $\Delta\delta_{S\text{-}R}$ values for the Mosher esters **3a** and **3b**.

as the link due to correlations from H-10 and H_3-22. Mutual HMBC correlations between olefinic H-13 and H-15 and their respective carbons combined with their additional correlation to the upfield quaternary center C-14 (δ_C 44.3) indicated that C-14 was the link to the fourth spin system. Correlation from the isolated CH_3-23 methyl group to C-14 established its position. Quaternary C-16 (δ_C 133.4) was assigned due to HMBC correlations from H-17, H-18b, H_3-24, and H_3-25. Fourth spin system protons H-15, H-17, H_2-18 and the isolated methyl H_3-23 correlated to the downfield quaternary carbon C-19 (δ_C 89.2), placing it adjacent to CH_2-18, indicating a bond to quaternary C-14 and thus a cyclohexene ring. The ketone carbonyl at C-20 (δ_C 196.0) was assigned adjacent to C-19 due to correlations from CH_2-18. The chemical shift of C-19 suggested oxidation, which implicated it as the quaternary center of a spirotetronate system due to its inclusion in the cyclohexene ring. C-1 (δ_C 169.3) and C-2 (δ_C 100.8) were assigned based on their chemical shifts since no protons were within HMBC correlation distance to them.

The NOESY spectrum (Table 1) revealed an NOE correlation between methylene proton H-18a and the H_3-23 isolated methyl group, providing additional support for the presence of the cyclohexene ring. The transannular NOE correlation between olefinic methine H-10 and oxymethylene H_2-21 was indicative of the macrocycle in **1**. Key NOESY interactions are shown in Figure 3b. Taken together, the NMR data were consistent with the X-ray crystal structure. The absolute configuration of **1** was confirmed by preparing (*S*)-MTPA (**3a**) and (*R*)-MTPA (**3b**) esters (Figure 3c).[21]

(21) (a) Dale, J. A.; Mosher, H. S. *J. Am. Chem. Soc.* **1973**, *95*, 512–519. (b) Ohtani, I.; Kusumi, T.; Kashman, Y.; Kakisawa, H. *J. Am. Chem. Soc.* **1991**, *113*, 4092–4096.

TABLE 2. ^{1}H, ^{13}C, gCOSY, and HMBC Data[e] for Spirohexenolide B (2) in C_6D_6

C/H no.	δ_H mult (*J*, Hz)[a]	δ_C (mult)[b]	COSY[c]	HMBC[c,d]
1		168.9 (C)		
2		101.1 (C)		
3		165.5 (C)		
4	7.59 d (10.0)	119.3 (CH)	5	3,6
5	6.20 d (10.0)	142.2 (CH)	4,21b	3,6,7,21
6		128.8 (C)		
7	4.97 t (8.5)	135.4 (CH)	8,21a	
8	1.53 m	27.8 (CH_2)	7,9a,9b	
9a	1.92 m	32.3 (CH_2)	8,9b,10	
9b	1.40 m		8,9a,10	
10	5.16 ddd (4.9, 10.9, 15.4)	125.3 (CH)	9a,9b,11	12
11	5.46 d (15.4)	139.7 (CH)	10	13,22
12		135.5 (C)		
13	5.13 s	134.8 (CH)	22	11,14,15,22,23
14		44.5 (C)		
15	5.33 s	129.0 (CH)	17,24	17,19,24
16		133.3 (C)		
17	2.10 m	33.9 (CH)	15,18a,18b,25	16,25
18a	2.30 dd (8.6, 14.6)	33.7 (CH_2)	17,18b	14,17,19,20,25
18b	1.62 d (14.6)		18a	14,16,17,19,20,25
19		88.4 (C)		
20		195.3 (C)		
21a	4.13 d (12.6)	63.4 (CH_2)	5,21b	3,5,6,7
21b	3.72 d (12.6)		7,21a	6,7
22	1.96 s	14.6 (CH_3)	13	11,12
23	1.30 s	27.4 (CH_3)		13,14,15,19
24	1.65 s	22.0 (CH_3)	15	15,16,17
25	1.43 d (6.9)	19.9 (CH_3)	17	16,17

[a] ^{1}H NMR data were collected at 500 MHz. [b] ^{13}C NMR data were collected at 125 MHz. [c] gCOSY and HMBC spectra were collected at 800 MHz. [d] The HMBC spectrum was collected with an evolution delay of $^{2,3}J_{CH}$ = 6 Hz. [e] Spectra were collected at 296 K in C_6D_6. Due to a slow decomposition of **2** in $CDCl_3$, C_6D_6 was required for extended times required to collect ^{13}C NMR, HMBC, and HSQC data.

With structure elucidation studies complete, we returned to culturing to produce additional quantities of compound **1** for biological studies. Using our optimized strains, we screened for media that provided an optimal yield of **1**. After evaluating over 50 different liquid cultures, we found that culturing *S. platensis* MJ1A in a fermentation media (6% w/v soluble starch, 1% w/v dry yeast, 1% w/v β-cyclodextrin, 1% w/v $CaCO_3$) containing 2% of Amberlite XAD-16 resin provided **1** at up to 325 mg/L (see the Experimental Section for further details). By increasing the resin content to 10%, we were able to obtain 15−20 mg/L of a second metabolite spirohexenolide B (**2**) from these cultures. The structure of **2** was characterized by X-ray crystallography (Figure 2) and subsequent NMR analyses (Table 2) indicating that **2** failed to undergo oxidation at C-8, suggesting that **2** is a biosynthetic precursor to **1**.

With access to the natural product, we were able to characterize its biological activity. While we identified **1** using an antibiotic screen, the activity of **1** was more significant in tumor cell lines. Initial activity studies used the human colon tumor HCT-116 cell line, and **1** displayed cytotoxicity activity with a GI_{50} value of 36.0 ± 5.1 μM, using the MTT assay. Submission of **1** to the single and multiple dose screens NCI-60 human tumor cell line screen[22] identified the enhanced activity as given by lower GI_{50} values in leukemia (CCRF-CEM, MOLT-4, and RPMI-8226), lung cancer (HOP-92), and colon cancer (SW-629) cell lines (complete data provided in the Supporting Information). Subsequent COMPARE analysis failed to provide a match to a known compound and any associated mechanism of action, suggesting a novel anticancer action for **1**. In vivo studies in athymic nude mice produced toxicity after a single dose of **1** (6−10 mg/kg), indicating the threshold for further studies.

We then turned to evaluate the cellular uptake and localization of **1** in HCT-116 tumor cells using fluorescence microscopy. Fortunately, spirohexenolide A (**1**) was natively fluorescent, with an excitation maximum λ_{max} = 435 nm and emission maximum at λ_{max} = 466 nm. HCT-116 cells were treated with 10 μM **1** in DMEM containing 10% FCS, 100 U/mL penicillin-G, and 100 μg/mL streptomycin and analyzed by fluorescence microscopy. Spirohexenolide A (**1**) was readily uptaken and appeared within minutes throughout the cell (Figure 4a). Within 6−12 h, fluorescence from **1** concentrated within vesicles surrounding the nucleus and remained in these structures (Figure 4b). This staining could not be washed from the cells by repetitive incubation with media and remained consistent thereafter (Figure 4c). Co-staining experiments with a panel of organelle probes provided a direct correlation with LysoTracker Red DND-99[23] (Figures 4d-4e) indicating that the localization occurred in the lysosomes.

Discussion

Spirohexenolide A (**1**) belongs to a large class of spirotetronate natural products that includes A88696F,[24] abyssomicins,[25] chlorothricin,[26] decatromicins,[27] pyrrolosporin A,[28]

(22) Shoemaker, R. H. *Nat. Rev. Cancer* **2006**, *6*, 813–823.
(23) Lemieux, B.; Percival, M. D.; Falgueyret, J. P. *Anal. Biochem.* **2004**, *327*, 247–251.
(24) Bonjouklian, R. *Tetrahedron Lett.* **1993**, *34*, 7861–7864.
(25) Bister, B.; Bischoff, D.; Ströbele, M.; Riedlinger, J.; Reicke, A.; Wolter, F.; Bull, A. T.; Zähner, H.; Fiedler, H. P.; Süssmuth, R. D. *Angew. Chem., Int. Ed.* **2004**, *43*, 2574–2576.
(26) Brufani, M.; Cerrini, S.; Muntwyle, R.; Fedeli, W.; Mazza, F. *Helv. Chim. Acta* **1972**, *55*, 2094–2102.
(27) Momose, I.; Hirosawa, S.; Nakamura, H.; Naganawa, H.; Iinuma, H.; Ikeda, D.; Takeuchi, T. *J. Antibiot.* **1999**, *52*, 787–796.
(28) Schroeder, D. R.; Colson, K. L.; Klohr, S. E.; Lee, M. S.; Matson, J. A.; Brinen, L. S.; Clardy, J. *J. Antibiot.* **1996**, *49*, 865–872.

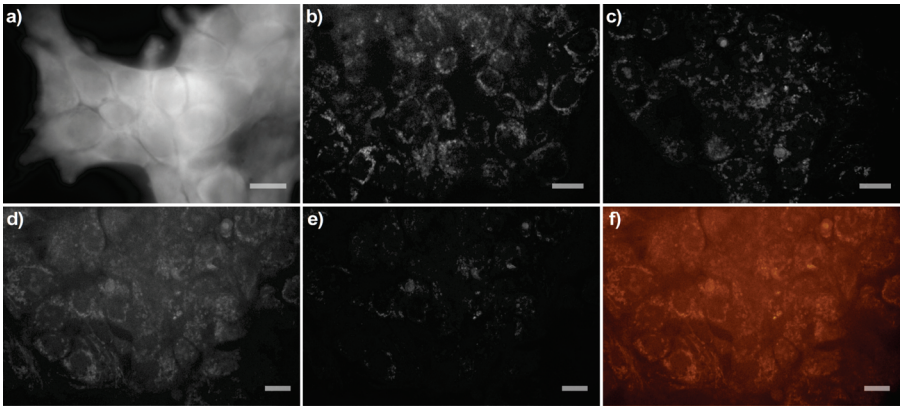

FIGURE 4. Uptake and subcellular localization of spirohexenolide A (**1**) in HCT-116 cells. Confocal fluorescent images from HCT-116 cells treated with 10 μM **1** for (a) 1 h, (b) 6 h, and (c) 12 h. Cells were washed twice with media prior to imaging. Live cell images were collected with excitation from a laser at 488 nm (emission filtered at 524 ± 40 nm). Co-staining with LysoTracker Red DND-99 indicates that compound **1** localizes within the lysosomes. HCT-116 cells were treated with 10 μM **1** for 6 h and washed before staining with 10 μM LysoTracker Red DND-99[23] for 20 min. (d) Fluorescence from **1** collected with excitation from a laser at 488 nm (emission filtered at 524 ± 40 nm). (e) Fluorescence from LysoTracker Red DND-99 collected with excitation from a laser at 568 nm (emission filtered at 624 ± 40 nm). (f) Two-color overlap depicting the fluorescence from **1** (red) and LysoTracker Red DND-99 (green). Yellow denotes overlap of both probes. Bars denote 10 μm.

PA-46101-A,[29] tetronomycin,[30] and versipelostatin.[31] While structural similarities exist, spirohexenolide A (**1**) contains a unique and functionally compact carbon framework and offers a new carbon skeleton. Its salient features include a unique pyran, a high degree of unsaturation, and a tetrasubstituted olefin juncture between its tetronic acid and the adjacent pyran. This juncture may be the result of an intramolecular dehydration reaction of an appropriately spaced distal alcohol onto the 3-keto portion of the spirotetronate, such as in carolic acid.[32]

The biosynthesis of **1** may be derived through a late-stage intramolecular Diels−Alder (IMDA) cycloaddition. Application of IMDA reactions to the syntheses of spirotetronate natural products is well established, such as in the total synthesis of abyssomicin C by Sorensen[33] and an approach to chlorothricolide by Yoshii.[34] To date, the biosynthetic gene clusters of four metabolites of this family (chlorothricin,[35] kijanimicin,[36] tetronomycin,[37] and tetrocarcin A[38]) have been elucidated and several of these pathways include a putative IMDA biogenesis. The isolation of spirohexenolide B (**2**) suggests that oxidation at C-8 arose at a late stage by oxidation via a cytochrome P450 or related enzyme.[39]

In conclusion, we have discovered two new spirotetronate polyketides, spirohexenolide A (**1**) and B (**2**), from *S. platensis*. We have elucidated their structures through spectroscopic and X-ray crystallographic analyses. We have shown that mutagenesis can be used in conjunction with culture optimization to provide viable quantities of trace metabolites.[40] Activity analyses indicated that **1** displayed significant activity against tumor cell growth with a unique specificity to select tumor cell lines (cf. NCI-60 cell line screening data in the Supporting Information). The fact that **2** (GI_{50} value of 61.2 ± 7.8 μM in HCT116 cells) also displayed comparable activity to **1** (GI_{50} value of 36.0 ± 5.1 μM in HCT116 cells) when screened in house using the MTT assay indicates that the C-8 hydroxyl group may serve as a site for reporter attachment for identifying its cellular targets.[41] The combination of the unique structure and activity of these spirohexenolides serve as the starting point for the development of both chemical synthesis and mechanism of action studies.

Experimental section

Mutagenesis of *S. platensis*. Spore suspensions were prepared from glycerol stocks of *S. platensis* MJ. While a series of strains were examined, we have only obtained compounds **1** and **2** from this parent strain and its mutants. A 1 μL aliquot of these suspensions was added to 1 mL of sterilized water and further diluted by addition of 10 μL of this solution into 10 mL of water to yield a solution containing approximately 6×10^5 spores/mL. This solution was then poured onto a sterile 9 cm glass Petri dish

(29) Matsumoto, M.; Kawamura, Y.; Yosimura, Y.; Terui, Y.; Nakai, H.; Yoshida, T.; Shoji, J. *J. Antibiot*. **1990**, *43*, 739–747.
(30) Keller-Juslén, C.; King, H. D.; Kuhn, M.; Loosli, H. R.; Pache, W.; Petcher, T. J.; Weber, H. P.; Von Wartburg, A. *J. Antibiot*. **1982**, *35*, 142–150.
(31) Park, H. R.; Chijiwa, S.; Furihata, K.; Hayakawa, Y.; Shin-Ya, K. *Org. Lett*. **2007**, *9*, 1457–1460.
(32) Clutterbuck, P. W.; Raistrick, H.; Reuter, F. *Biochem. J*. **1935**, *29*, 300–321.
(33) Zapf, C. W.; Harrison, B. A.; Drahl, C.; Sorensen, E. J. *Angew. Chem., Int. Ed*. **2005**, *44*, 6533–6537.
(34) Takeda, K.; Igarashi, Y.; Okazaki, K.; Yoshii, E.; Yamaguchi, K. *J. Org. Chem*. **1990**, *55*, 3431–3434.
(35) Jia, X. Y.; Tian, Z. H.; Shao, L.; Qu, X. D.; Zhao, Q. F.; Tang, J.; Tang, G. L.; Liu, W. *Chem. Biol*. **2006**, *13*, 575–585.
(36) Zhang, H.; White-Phillip, J. A.; Melançon, C. E. 3rd; Kwon, H. J.; Yu, W. L.; Liu, H. W. *J. Am. Chem. Soc*. **2007**, *129*, 14670–14683.
(37) Demydchuk, Y.; Sun, Y.; Hong, H.; Staunton, J.; Spencer, J. B.; Leadlay, P. F. *ChemBioChem* **2008**, *9*, 1136–1145.
(38) Fang, J.; Zhang, Y.; Huang, L.; Jia, X.; Zhang, Q.; Zhang, X.; Tang, Z. *J. Bacteriol*. **2008**, *190*, 6014–6025.
(39) Related P450 oxidations: (a) Machida, K.; Aritoku, Y.; Tsuchida, T. *J. Biosci. Bioeng*. **2009**, *107*, 596–598. (b) Lin, X.; Cane, D. E. *J. Am. Chem. Soc*. **2009**, *131*, 6332–6333. (c) Henry, K. M.; Townsend, C. A. *J. Am. Chem. Soc*. **2005**, *127*, 3724–3733.
(40) Bode, H. B.; Bethe, B.; Hofs, R.; Zeeck, A. *ChemBioChem* **2002**, *3*, 619–627.
(41) (a) Hughes, C. C.; MacMillan, J. B.; Gaudêncio, S. P.; Fenical, W.; La Clair, J. J. *Angew. Chem., Int. Ed*. **2009**, *48*, 728–732. (b) Leslie, B. J.; Hergenrother, P. J. *Chem. Soc. Rev*. **2008**, *37*, 1347–1360. (c) Alexander, M. D.; Burkart, M. D.; Leonard, M. S.; Portonovo, P.; Liang, B.; Ding, X.; Joullié, M. M.; Gulledge, B. M.; Aggen, J. B.; Chamberlin, A. R.; Sandler, J.; Fenical, W.; Cui, J.; Gharpure, S. J.; Polosukhin, A.; Zhang, H. R.; Evans, P. A.; Richardson, A. D.; Harper, M. K.; Ireland, C. M.; Vong, B. G.; Brady, T. P.; Theodorakis, E. A.; La Clair, J. J. *ChemBioChem* **2006**, *7*, 409–416.

and UV irradiated (Stratalinker 1800) at 8000 μJ at a distance of 12 cm while being stirred. Samples were taken every 6 s over a 3 min period. After serial dilution of UV-irradiated spore suspension in deionized H_2O, the sample was spread onto Bennett's agar (1.0% w/v glucose, 0.2% w/v pancreatic digest of casein, 0.1 w/v of yeast extract, 0.1% w/v beef extract, 1.5% w/v of agar in deionized H_2O at pH 7.0), YEMED agar (0.4% w/v yeast extract, 1.0% w/v malt extract, 0.4% w/v glucose, 1.5% w/v agar in deionized H_2O at pH 7.2), and ISP4 agar (1.0% w/v soluble starch, 0.2% w/v $CaCO_3$, 0.1% w/v K_2HPO_4, 0.1% w/v $MgSO_4 \cdot 7H_2O$, 0.1% w/v NaCl, 0.2% w/v $(NH_4)_2SO_4$, 0.001% w/v $FeSO_4 \cdot 7H_2O$, 0.001% w/v $MnCl_2 \cdot 4H_2O$ and 0.001% w/v of $ZnSO_4 \cdot 7H_2O$ in deionized H_2O at pH 7.2) for examining the morphologically differentiating colonies. To prevent photoreactivation, the plates were wrapped with foil for 24 h and then incubated at 30 °C for 15 days.

Mutant Screening Identifies Producer Strains *S. platensis* MJ1A1 and MJ1A2. After 15 days of incubation, survival colonies were transferred onto R2YE media (10.3% w/v sucrose, 0.5% w/v yeast extract (Difco), 0.01% w/v casaminoacids (Difco), 0.025% w/v K_2SO_4, 1.01% w/v $MgCl_2 \cdot 6H_2O$, 1% w/v glucose, 0.025% w/v KH_2PO_4, 0.29% w/v $CaCl_2 \cdot 2H_2O$, 0.0008% w/v $ZnCl_2$, 0.004% w/v $FeCl_3 \cdot 6H_2O$, 0.0004% w/v $CuCl_2 \cdot 2H_2O$, 0.0004% w/v $MnCl_2 \cdot 4H_2O$, 0.0004% w/v $Na_2B_4O \cdot 10H_2O$, 0.0004% w/v $(NH_4)_5Mo_7O_{24} \cdot 4H_2O$ 0.3% w/v L-proline, 0.573% w/v *N*-tris(hydroxymethyl)methyl-2-aminoethane-sulfonic acid (TES), 0.005% v/v 1 N NaOH to provide a pH 7.2). Once the mutants had sporulated, agar cones (3 mm OD × 5 mm height) were excised containing a single colony and stamped on top of a glucose basal salt (1% g of glucose, 0.01% yeast extract, 1.5% agar, 0.02% $MgSO_4 \cdot 7H_2O$, 0.001% NaCl, 0.001% $FeSO_4 \cdot 7H_2O$, 0.001% $MnSO \cdot 4H_2O$ 0.2% NH_4Cl, 0.465% K_2HPO_4, 0.09% of KH_2PO_4 at pH 7.0) agar seeded with $\sim 8 \times 10^7$ of *Bacillus subtilis* 6633 per cm^2. After incubation at 37 °C for 24 h, colonies showing a zone of inhibition were compared against their parent strain. Strains MJ1A, MJ2B and MJ6 (Figure 1a) were obtained with this method.

Minimum Inhibitory Concentration (MIC) Assay of Spirohexenolide A (1), using *Bacillus subtilis* 6633. Spirohexenolide A (**1**) in dimethyl sulfoxide (DMSO) was diluted to 10, 15, 30, 60, 120, 250, 500, and 1000 μg/mL stocks in tryptic soy broth with a final concentration of 1% DMSO. *B. subtilis*, cultured for 18 h at 37 °C in tryptic soy broth, was inoculated at 1/10 000 to a final volume of 200 μL per well on a 96 well plate and then treated with 2 μL of a stock solution of **1** (10, 15, 30, 60, 120, 250, 500, and 1000 μg/mL in tryptic soy broth containing 1% DMSO). The plate was incubated in 37 °C for 18 h, indicating that pure **1** had an MIC value of 12.25 μM (no visible bacterial growth). The compound was tested in duplicates. Negative control comprised of DMSO solvent did not show any effect on the bacterial growth.

Culturing of Spirohexenolide A (1) from *S. platensis* Strain MJ1A1. A single colony of *S. platensis* MJ1A1 grown on yeast extract-malt extract-dextrose (YEMED) agar was resuspended in 50 μL of sterilized water, using a sterilized pellet pestle, and inoculated into 3 mL of tryptic soy broth (BD Biosciences) and shaken at 220 rpm at 28 °C for 40 h. An aliquot (2 mL) of this starter culture was transferred into a 250 mL baffled Erlenmeyer flask containing 100 mL of seed medium containing 1% w/v glucose, 2.4% w/v soluble starch, 0.3% w/v beef extract, 0.5% w/v tryptone, 0.5% w/v yeast extract, and 2.0% w/v $CaCO_3$ adjusted to pH 7.2. After shaking the seed medium for 48 h at 220 rpm and 28 °C, a 50 mL aliquot was transferred to a 2.8 L baffled Erlenmeyer flask containing 500 mL of fermentation media (6% w/v soluble starch, 1% w/v dry yeast, 1% w/v β-cyclodextrin, 0.2% w/v $CaCO_3$ adjusted to pH 6.8 prior to sterilization) and 2% w/v of Amberlite XAD-16 resin (Alfa Aesar) that was washed repetitively with deionized water prior to sterilization. The fermentation media was shaken for 72 h at 220 rpm at 28 °C. The cultures were filtered through cheesecloth to collect the resin. The resin was then returned to the baffled flask and acetone (250 mL) and EtOAc (250 mL) were added. The flask was shaken for 2 h at 220 rpm. The resin was filtered again through cheesecloth, and the filtrate was concentrated on a rotary evaporator until only insoluble solids and water remained. EtOAc was added until most of the solids were dissolved, and the mixture was poured into a separatory funnel. The aqueous layer was extracted with additional EtOAc (2 × 100 mL), and the combined organic layers were concentrated to provide a crude extract. Crude extract was dissolved in a minimum amount of 1:1 hexanes:EtOAc (sonication was used to facilitate dissolution). A 2 in. ID column containing silica gel (EM Sciences) was packed with 1:1 hexanes:EtOAc, and the solution of the crude extract was loaded. The column was run with 1:1 hexanes:EtOAc for at least two column volumes before EtOAc was used to elute **1** with R_f 0.29 (EtOAc). Compounds **1** and **2** could be visualized by ceric ammonium molybdate, 2,4-dinitrophenylhydrazine, iodine, and potassium permanganate stains, and short-wave UV (excitation at 254 nm). Pure spirohexenolide A (**1**) was obtained after a second flash column, using a gradient from hexanes to EtOAc or trituration with small amounts of absolute ethanol.

Isolation of Spirohexenolide B (2) from Cultures of *S. platensis* Strain MJ1A1. *S. platensis* strain MJ1A1 was cultured in the same manner on the same scale used to produce spirohexenolide A (**1**), (above), but the fermentation media was supplemented with 10% w/v of Amberlite XAD-16 resin (Alfa Aesar) that was washed repetitively with deionized water prior to sterilization. The fermentation media was shaken for 72 h at 220 rpm at 28 °C. The crude extract of the resin was processed in the same manner as used for the isolation of spirohexenolide A (**1**), as described in the preceding paragraph. A 2 in. i.d. column containing silica gel (EM Sciences) was packed with 1:1 hexanes:EtOAc, and the solution of the crude extract was loaded. The column was run with 1:1 hexanes:EtOAc for two column volumes, and spirohexenolide B (**2**) was obtained from the eluted and concentrated material by subjecting it to a second Flash purification on a 2 in. i.d. column with a gradient from hexanes to 1:1 hexanes:EtOAc with elution of **2** in 1:1 hexanes:EtOAc with R_f 0.68 (EtOAc), followed by crystallization from either EtOH or a mixture of CH_2Cl_2 and hexanes to obtain yellow crystals.

Synthesis of Mosher Esters 3a and 3b. The (*S*)- and (*R*)-MTPA derivatives **3a** and **3b** were prepared with use of a slight modification of the standard procedure.[21] (*S*)-MTPA ester **3a**: To a sample of compound **1** (30.3 mg, 0.0743 mmol) in a dry 25 mL round-bottomed flask with a Teflon-coated magnetic stirbar were added a few crystals of 4-dimethylaminopyridine and the flask was sealed with a rubber septum and flushed with argon. CH_2Cl_2 (3 mL) and pyridine (0.120 mL, 1.5 mmol) were added at rt, and the mixture was stirred until a yellow solution was achieved. Stirring was then continued as 70 μL of (*R*)-MTPA-Cl (0.374 mmol) was added via syringe at rt. After 30 min the solution turned dark green. After 50 min, TLC indicated a new compound had formed with R_f 0.76 (EtOAc), and that compound **1** had been consumed. The reaction mixture was then poured into a separatory funnel containing half-saturated $NaHCO_3$ (30 mL) and CH_2Cl_2 (20 mL), and the organic layer became yellow again upon shaking. The aqueous layer was extracted with another 20 mL of CH_2Cl_2 and the combined organic layers were dried over Na_2SO_4 and concentrated under reduced pressure. The residue was dissolved in 3:1 hexanes:EtOAc (5 mL), and standard flash chromatography with 3:1 hexanes:EtOAc provided pure **3a** (16.3 mg, 35%). The same procedure was used on **1** and (*S*)-MTPA-Cl to make the (*R*)-MTPA ester **3b** (13.5 mg, 40%).

Spirohexenolide A (1):. yellow needles, mp 280−285 °C dec; $[\alpha]^{25}_D$ +551.3 (*c* 0.4, $CHCl_3$); UV λ_{max} (MeOH) 339 (ε 8650), 236

(ε 25583) nm; IR (film) ν_{max} 3469, 1754, 1702, 1582, 1550, 1059, 1043, 988, and 968 cm^{-1}; ESIMS *m/z* 409.03 $[M + H]^+$, 431.03, $[M + Na]^+$; HR-EI-MS *m/z* 408.1947, $[M]^+$ (calcd for $C_{25}H_{28}O_5$ $[M]^+$, 408.1931); ^1H and ^{13}C NMR (Table 1).

Spirohexenolide B (2):. yellow rhomboid crystals recrystallized from CH_2Cl_2 and hexanes, mp 219−221 °C dec; IR (film) ν_{max} 2922, 2852, 1735, 1707, 1587, 1551, 1466, 1410 cm^{-1}; ESIMS *m/z* 392.91 $[M + H]^+$; HR-ESI-MS *m/z* 415.1888, $[M + Na]^+$ (calcd for $C_{25}H_{28}O_4Na$ $[M + Na]^+$, 415.1885); ^1H and ^{13}C NMR (Table 2).

Spirohexenolide A (*S*)-MTPA derivative (3a):. yellow solid, mp 208−211 °C dec; $[\alpha]^{23}_D$ +159.3 (*c* 1, CH_2Cl_2); IR (film) ν_{max} 2936, 1750, 1709, 1594, 1554, 1252, 1168, 1056, 1014, and 722 cm^{-1}; ESI-MS *m/z*: 624.92 $[M + H]^+$, 647.04 $[M + Na]^+$; HR-ESI-FT-MS (Orbit-trap-MS) *m/z* calcd for $C_{35}H_{35}F_3O_7Na$ $[M + Na]^+$ 647.2227, found 647.2218; see the Supporting Information for ^1H and ^{13}C NMR spectroscopic data.

Spirohexenolide A (*R*)-MTPA derivative (3b):. yellow solid, mp 246−250 °C dec; $[\alpha]^{23}_D$ +223.5 (*c* 1, CH_2Cl_2); IR (film) ν_{max} 2936, 1750, 1709, 1594, 1554, 1252, 1169, 1056, and 1014 cm^{-1}; ESI-MS *m/z*: 625.18 $[M + H]^+$, 647.21 $[M + Na]^+$; HR-ESI-FT-MS (Orbit-trap-MS) *m/z* calcd for $C_{35}H_{36}F_3O_7$ $[M + H]^+$ 625.2408, found 625.2419; see the Supporting Information for ^1H and ^{13}C NMR spectroscopic data.

Uptake and Localization in HeLa Cells. HCT-116 cells (ATCC CCL-247) were cultured in Dulbecco′s modification of Eagle′s medium (DMEM) with 4.5 g L^{-1} glucose, 4.5 g L^{-1} L-glutamine, and 5% heat inactivated fetal calf serum (FCS) in glass-bottom dishes. Fluorescent images were collected on a Leica (Wetzlar, Germany) DMI6000 inverted confocal microscope with a Yokogawa (Tokyo, Japan) spinning disk confocal head, Orca ER High Resolution B&W Cooled CCD camera (6.45 μm/pixel at 1X) (Hamamatsu, Sewickley, PA), Plan Apochromat 40×/1.25 na and 63×/1.4 na objective, and a Melles Griot (Carlsbad, CA) Argon/Krypton 100 mW air-cooled laser for 488, 568, and 647 nm excitations. Confocal z-stacks were acquired in all experiments. Co-staining was conducted by treating cells exposed to **1** to either Syto 60 (nucleus), LysoTracker Red DND-99 (lysosomes), BODIPY TR glibenclamide (endoplasmic reticulum), or MitoTracker Red 580 (mitochondria) for 20 min and washing the cells three times with media and collecting images in two colors.

X-ray Crystallography. A yellow needle of compound **1** 0.25 × 0.10 × 0.10 mm^3 in size was mounted on a Cryoloop with Paratone oil. Data were collected in a nitrogen gas stream at 100(2) K using ψ and ω scans. Crystal-to-detector distance was 50 mm and exposure time was 10 s per frame with a scan width of 0.5°. Data collection was 99.3% complete to 67.00° in θ. A total of 7195 reflections were collected covering the indices, $-8 \leq h \leq 8$, $-15 \leq k \leq 14$, $-13 \leq l \leq 13$. A total of 3065 reflections were found to be symmetry independent, with an R_{int} of 0.0366. Indexing and unit cell refinement indicated a primitive, monoclinic lattice. The space group was found to be *P*2(1) (No. 4). The data were integrated with the Bruker SAINT software program and scaled with the SADABS software program. Solution by direct methods (SIR-2004) produced a complete heavy-atom phasing model consistent with the proposed structure. All non-hydrogen atoms were refined anisotropically by full-matrix least-squares (SHELXL-97). All hydrogen atoms were placed with use of a riding model. Their positions were constrained relative to their parent atom by using the appropriate HFIX command in SHELXL-97.

A colorless plate of compound **2** 0.33 × 0.28 × 0.08 mm^3 in size was mounted on a Cryoloop with Paratone oil. Data were collected in a nitrogen gas stream at 100(2) K, using ψ and ω scans. Crystal-to-detector distance was 50 mm and exposure time was 10 s per frame with a scan width of 0.5°. Data collection was 99.9% complete to 25.00° in θ. A total of 24117 reflections were collected covering the indices, $-8 \leq h \leq 8$, $-15 \leq k \leq 15$, $-27 \leq l \leq 27$. A total of 7549 reflections were found to be symmetry independent, with an R_{int} of 0.0363. Indexing and unit cell refinement indicated a primitive, monoclinic lattice. The space group was found to be *P*2(1). The data were integrated with the Bruker SAINT software program and scaled with the SADABS software program. Solution by direct methods (SIR-2004) produced a complete heavy-atom phasing model consistent with the proposed structure. All non-hydrogen atoms were refined anisotropically by full-matrix least-squares (SHELXL-97). All hydrogen atoms were placed with use of a riding model. Their positions were constrained relative to their parent atom by using the appropriate HFIX command in SHELXL-97.

Acknowledgment. Financial support from the American Cancer Society (RSG-06-011-01-CDD) is gratefully acknowledged. We thank Dr. Yongxuan Su (UC San Diego) for mass spectrometric analyses, and Drs. Anthony Mrse and Xuemei Huang (UC San Diego) for assistance with acquiring the NMR data.

Supporting Information Available: ^1H, ^{13}C, DEPT, gCOSY, TOCSY, NOESY, ROESY, HSQC, and HMBC spectra on spirohexenolide A (**1**), ^1H, ^{13}C, DEPT, gCOSY, TOCSY, NOESY, ROESY, HSQC, and HMBC spectra on spirohexenolide B (**2**), ^1H, ^{13}C spectra of **3a** and **3b**, copies of crystallographic information files (CIF) for compounds **1** and **2**, as well as copies of the NCI data on spirohexenolide A (**1**). This material is available free of charge via the Internet at http://pubs.acs.org.